Hyperfine Interact (2015) 231:65–74
DOI 10.1007/s10751-014-1086-8

^{57} Fe Mössbauer and magnetic studies of $Nd_3Fe_{24.5}Cr_{4.5}$

**J. L. Wang · M. F. Md Din · S. J. Campbell ·
S. J. Kennedy · F. M. Yang · G. H. Wu ·
S. X. Dou**

Received: 2 October 2014 / Accepted: 14 October 2014 / Published online: 14 November 2014

Abstract The structural and magnetic properties of the rare earth transition metal compound $Nd_3Fe_{24.5}Cr_{4.5}$ have been investigated by variable temperature high resolution x-ray diffraction together with DC magnetization and ^{57}Fe Mössbauer effect measurements. The magnetic ordering temperature has been found to be $T_C = 423(5)$ K with spin reorientation detected below room temperature around $T_{sr} = 158(5)$ K. Rietveld refinements indicate that $Nd_3Fe_{24.5}Cr_{4.5}$ crystallizes in the $Nd_3(Fe,Ti)_{29}$-type structure with the A2/m space group and a substantial magneto-volume effect is detected around T_C. The Mössbauer spectra can be fitted well using five sub-spectra. The temperature dependence of the average hyperfine field has been analysed in terms of different power laws of the reduced temperature. The Debye temperature of $Nd_3Fe_{24.5}Cr_{4.5}$ has been determined as $\theta_D = 400(\pm 30)$ K from a fit to the variable temperature isomer shift IS(T).

Keywords Rare earth compound · Magneto-volume · Mössbauer spectroscopy · Magnetic phase transition

---

Proceedings of the 5th Joint International Conference on Hyperfine Interactions and International Symposium on Nuclear Quadrupole Interactions (HFI/NQI 2014) Canberra, Australia, 21-26 September 2014

J. L. Wang · M. F. Md Din · S. X. Dou
Institute for Superconductivity and Electronic Materials, University of Wollongong, Wollongong, NSW 2522, Australia

J. L. Wang · S. J. Kennedy
Bragg Institute, ANSTO, Lucas Heights, NSW 2234, Australia

S. J. Campbell (✉)
School of Physical, Environmental and Mathematical Sciences, The University of New South Wales, Canberra, ACT 2600, Australia
e-mail: stewart.campbell@adfa.edu.au

F. M. Yang · G. H. Wu
Institute of Physics, Chinese Academy of Science, Beijing 100190, People's Republic of China

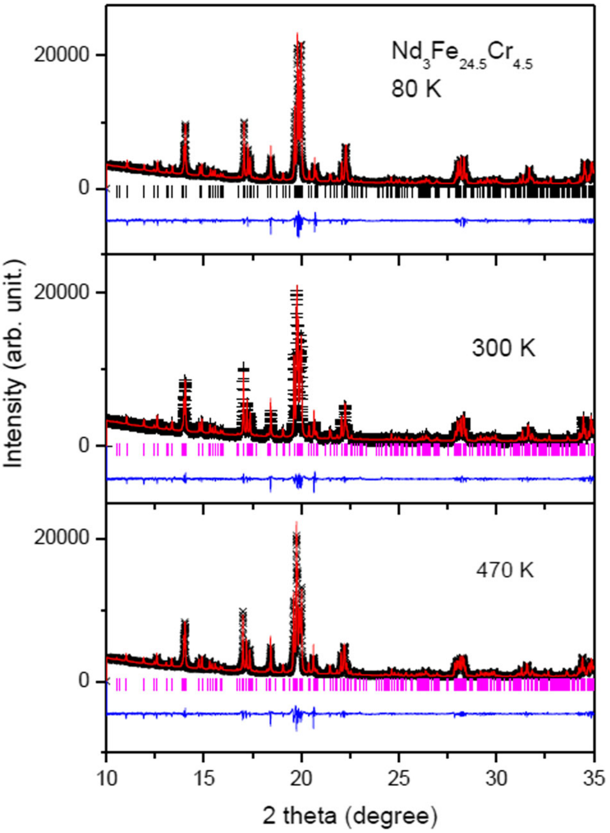

Fig. 1 X-ray diffraction patterns of $Nd_3Fe_{24.5}Cr_{4.5}$ at T = 80 K, 300 K and 470 K ($\lambda = 0.7288$ Å). The Rietveld refinements are shown with markers for the $Nd_3(Fe,Ti)_{29}$-type structure (A2/m space group) along with the difference between the data and the fit

1 Introduction

Since the discovery of the rare-earth iron-rich $R_3(Fe,T)_{29}$ series of compounds (R stands for rare earth element or Y; T is a stabilizing element such as Ti, Mo, V, Cr, etc) [1], compounds based on this series have continued to attract strong interest [2] in the search for high performance permanent-magnet materials. The $R_3(Fe,T)_{29}$ compounds crystallize in the monoclinic system of $A2/m$ space group with two formula units per cell consisting of alternate stacking tetragonal $ThMn_{12}$-type (1:12) and rhombohedral Th_2Zn_{17}-type (2:17 R) segments [3–5]. Among them, the $Sm_3(Fe,Ti)_{29}N_y$ [7] and $Sm_3(Fe,Ti)_{29}C_y$ [8] compounds with strong uniaxial anisotropy and high-saturation magnetization were considered as potential candidates for applications as permanent magnets. Moreover, it was also found that $Gd_3(Fe_{1-x}Co_x)_{29-y}Cr_y$compounds possess easy-axis-type anisotropy at room temperature for $x > 0.4$ [9, 10].

A large spontaneous magnetostriction and Invar-like behavior in the thermal expansion coefficient have been observed in the vicinity of T_C in these $R_3(Fe,T)_{29}$ series [11–13] The thermal expansion anomaly observed below the ordering temperature was proposed to be a result of the strong dependence of the magnetic interactions with the interatomic distances

Table 1 Bond lengths in $Nd_3Fe_{24.5}Cr_{4.5}$ at 300 K

Atom	# of Nd neighbours	# of Fe neighbours	WZV-Volume (Å^3)	Minimum bond length to neighbouring Fe (Å)	Maximum bond length to neighbouring Fe (Å)	Average bond length to neighbouring Fe (Å)
Nd-1, 2a	0	**20** (4× Fe-9, 2× Fe-4, 2× Fe-3, 2× Fe-5, 2× Fe-7, 4× Fe-2, 4× Fe-11)	30.858	3.003	3.277	3.1410
Nd-2, 4e	1 (1× Nd-2)	**19** (4× Fe-8, 2× Fe-9, 6× Fe-10, 2× Fe-5, 1× Fe-6, 1× Fe-4, 2× Fe-1,1× Fe-1)	31.816	3.067	3.346	3.1686
Fe-1, 2c	2 (1× Nd-2)	**10** (4× Fe-8, 4× Fe-10, 2× Fe-6)	11.252	2.398	2.688	2.4831
Fe-2, 4e	2(1× Nd-1)	**10** (2× F11, 2× Fe-4, 2× Fe-9, 2× Fe-7, 2× Fe-3)	11.387	2.411	2.646	2.5129
Fe-3, 4g	1(1× Nd-1)	**13**: 1× Fe-3, 2× Fe-11, 2× Fe-2, 2× Fe-4, 2× Fe-9, 2× Fe-7, 2× Fe-6	12.307	2.412	2.887	2.6735
Fe-4, 4i	2(1× Nd-1, 1× Nd-2)	**10**: 2× Fe-11, 2× Fe-2, 2× Fe-3, 1× Fe-6, 1× Fe-7, 2× Fe-9	11.710	2.421	2.711	2.5634
Fe-5, 4i	3(1× Nd-1, 2× Nd-2)	**9**: 2× Fe-11, 2× Fe-10, 2× Fe-8, 1× Fe-7,2× Fe-9	12.092	2.484	2.720	2.5741
Fe-6, 4i	1(1× Nd-2)	**13**: 1× Fe-7, 2× Fe-11,1× Fe-4, 2× Fe-9, 1× Fe-1, 2Fe-10, 2× Fe-8, 2× Fe-3	12.218	2.258	2.887	2.6645

Table 1 (continued)

Atom	# of Nd neighbours	# of Fe neighbours	WZV-Volume (Å^3)	Minimum bond length to neighbouring Fe (Å)	Maximum bond length to neighbouring Fe (Å)	Average bond length to neighbouring Fe (Å)
Fe-7, 4i	1(1× Nd-1)	**13**: 1× Fe-6, 2× Fe-2, 1× Fe-5, 2× Fe-9, 1× Fe-4, 2× Fe-8, 2× Fe-11, 2× Fe-13	12.413	2.258	2.867	2.6750
Fe-8, 8j	2(2× Nd-2) 1× Nd-2)	**11**: 1× Fe-1, 2× Fe-8, 1× Fe-9, 3× Fe-10, 1× Fe-11, 1× Fe-5, 1× Fe-7, 1× Fe-6	11.771	2.398	3.616	2.6680
Fe-9, 8j	2(1× Nd-1,	**11**: 2× Fe-11, 1× Fe-2, 1× F8, 1× Fe-10, 1× Fe-3, 1× Fe-7, 1× Fe-6, 1× Fe-4, 1× Fe-5, 1× Fe-9	11.652	2.379	3.746	2.6783
Fe-10, 8j	3(3× Nd-2)	**9**: 1× Fe-11, 1× Fe-1, 1× Fe-10, 3 × Fe-8, 1× Fe-5, 1× Fe-9, 1× Fe-6	11.996	2.442	2.722	2.5528
Fe-11, 8j	2(1× Nd-1, (1× Nd-2)	**10**: 2× Fe-9, 1× Fe-2, 1× Fe-4, 1× Fe-10, 1× Fe-5, 1× Fe-8, 1× Fe-6, 1× Fe-2, 1× Fe-7	11.302	2.379	2.730	2.5013

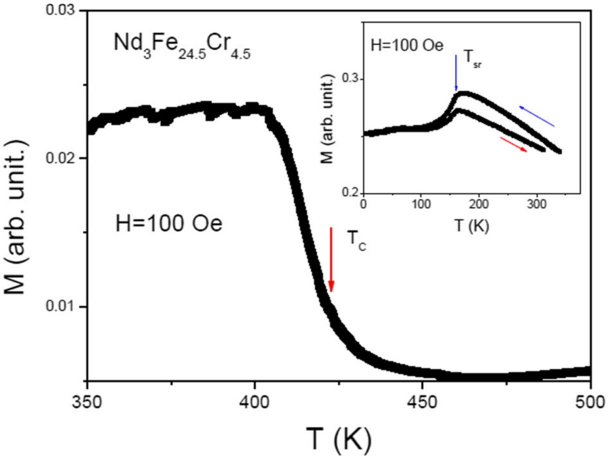

Fig. 2 The temperature dependence of the magnetization of $Nd_3Fe_{24.5}Cr_{4.5}$ as measured in a field of H = 100 Oe. The spin reorientation and Curie temperatures are derived as T_{sr} = 158(5) K and T_C = 423(5) K respectively

associated with a competition of interactions of opposite sign - positive for ferromagnetic and negative for antiferromagnetic).

In the present work we focus on the crystal structure and magnetic properties of $Nd_3Fe_{24.5}Cr_{4.5}$ using variable temperature high resolution x-ray diffraction at the Australian Synchrotron together with DC magnetization and ^{57}Fe Mössbauer effect measurements. The $Nd_3Fe_{24.5}Cr_{4.5}$ sample has been investigated over the temperature range ∼5 – 650 K.

2 Experiments

The $Nd_3Fe_{24.5}Cr_{4.5}$ sample was prepared by argon arc melting the constituent elements of purity ∼99.9 % followed by annealing in a sealed quartz tube under a protective argon atmosphere at 980 °C for three days. The crystal structure of the sample was checked by high intensity x-ray powder diffraction (λ = 0.7288 Å; 80 – 470 K) at the Australian Synchrotron. The magnetization was measured in a magnetic field of 0.01 T over the temperature range from 5 K to 650 K using the vibrating sample magnetometer option of a Quantum Design 14 T physical properties measurement system (PPMS). The ^{57}Fe Mössbauer spectra were obtained between 5 K and 300 K using a standard constant acceleration spectrometer and a ^{57}Co**Rh** source. The spectrometer was calibrated at room temperature with an α-iron foil.

3 Results and discussion

The x-ray diffraction patterns of $Nd_3Fe_{24.5}Cr_{4.5}$ at T = 80 K, 300 K and 470 K collected at the Australian Synchrotron are shown in Fig. 1a as typical examples. Rietveld refinements indicate that $Nd_3Fe_{24.5}Cr_{4.5}$ crystallizes in the $Nd_3(Fe,Ti)_{29}$-type structure with the A2/m space group as expected, and that no structural change occurs with variation in temperature from 80 K to 470 K. The lattice parameters at 300 K are derived to be a = 10.596(2) Å;

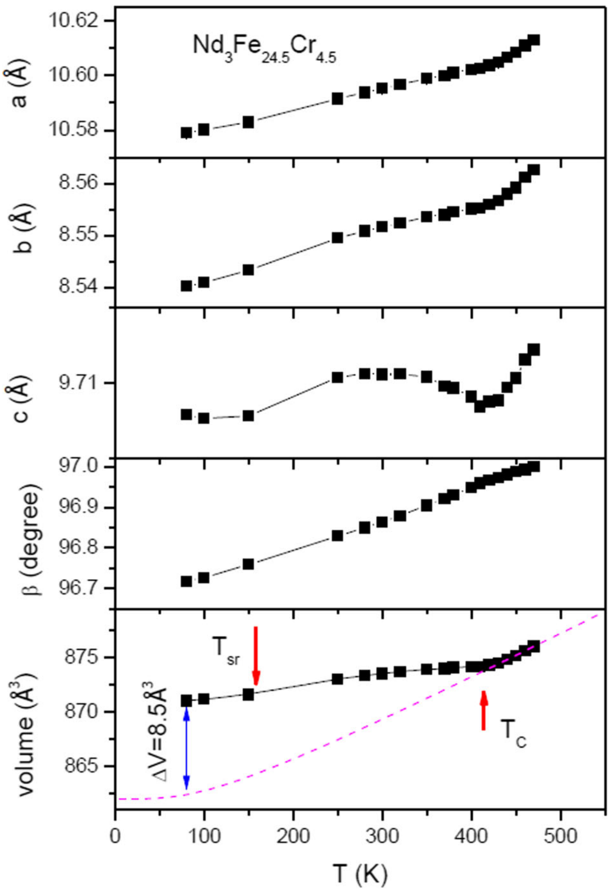

Fig. 3 Temperature dependences of the $Nd_3Fe_{24.5}Cr_{4.5}$ lattice parameters a, b, c, β, and V. The solid curves are guides to the eye while the dashed line in the graph of unit cell volume versus temperature represents the calculated lattice contribution using the Debye model as discussed in the text. The arrows indicate the Curie temperature T_C and spin reorientation temperature T_{sr}

b = 8.552(1) Å; c = 9.711(2) Å; β = 96.87(1); V = 873.76(5) Å^3, which are very close to the values reported by Han et al. [14] (where a = 10.615 Å; b = 8.556 Å; c = 9.714 Å; β = 96.9°). The pattern factor R_p, the weighted pattern factor R_{wp}, and the expected pattern factor R_{exp} are 4.99, 6.98 and 2.89, respectively. The bond lengths between different sites and the Wigner–Seitz cell (WSC) volume have been calculated with the BLOKJE program [15] using the structural and positional parameters and the 12-coordinate metallic radii of 1.82 Å, 1.26 Å and 1.3 Å for Nd, Fe and Cr, respectively (see Table 1). It can be seen that the minimum Fe–Fe bond length spanan interval from 2.258 Å to 2.484 Å. It is well accepted that for Fe-rich rare-earth compounds Fe moments with short bonds ($<$ 2.45 Å [16, 17]) are antiferromagnetically coupled while those with long bonds are ferromagnetically coupled. It is reasonable to conclude that two types of Fe-Fe exchange interaction co-exist in $Nd_3Fe_{24.5}Cr_{4.5}$ - positive (ferromagnetic) and negative (antiferromagnetic) - similar to both R_2Fe_{17}- based [18] and R(Fe,T)$_{12}$-based [19, 20] compounds. As such, this provides scope for further increases in their Curie temperatures by modifying the bond distances.

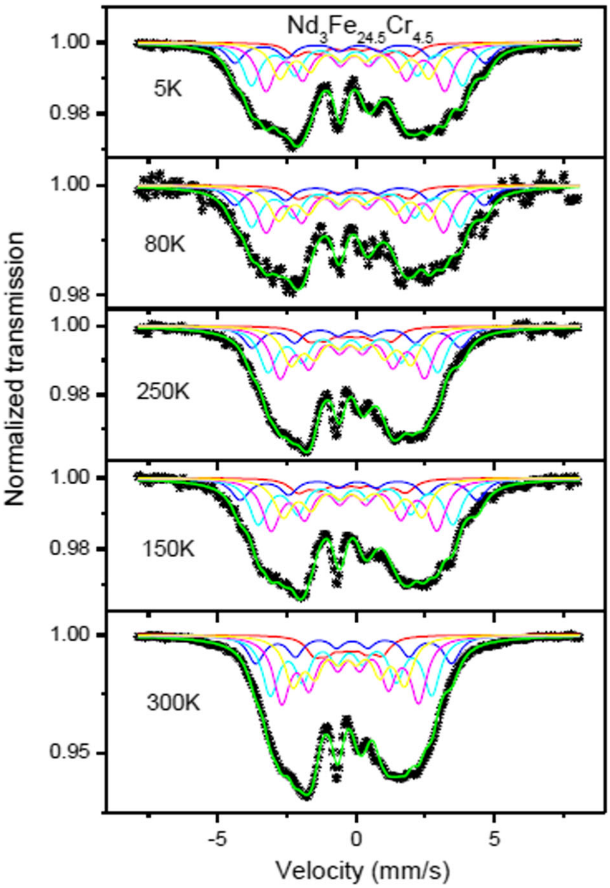

Fig. 4 Mössbauer spectra of $Nd_3Fe_{24.5}Cr_{4.5}$ at the temperatures indicated. The spectra were fitted using five sub-spectral components as described in the text and shown in the figure

The temperature dependence of the $Nd_3Fe_{24.5}Cr_{4.5}$ magnetization as measured in a field of 100 Oe is shown in Fig. 2. The spin reorientation temperature and Curie temperature are found to be $T_{sr} = 158(5)$ K and $T_C = 423(5)$ K, similar to the transition temperatures reported previously [14].

The temperature dependences of the a, b and c lattice parameters derived from Rietveld refinements are drawn in Fig. 3. The lattice parameter $c$is found to remain essentially invariant with increasing temperature up to around T_{sr}, before exhibiting an unusual broad peak centred around 300 K, between T_{sr} and T_C. The c lattice parameter exhibits a minimum value at T_C before increasing monotonically with further increase in temperature. On the other hand, the a and b lattice parameters decrease monotonically with decreasing temperature but both show distinct bend-like deviations around T_C (Fig. 3). These variations of the a, b and c lattice parameters with temperature are very similar to the behaviours observed in $Nd_3Fe_{26.5}Re_{2.5}$ compound [12] where there also exists a strong magneto-structural coupling in all directions.

In order to isolate the magnetic contribution to the thermal expansion, the lattice thermal contribution has been calculated using the Grüneisen relation [18–20]. This is demonstrated

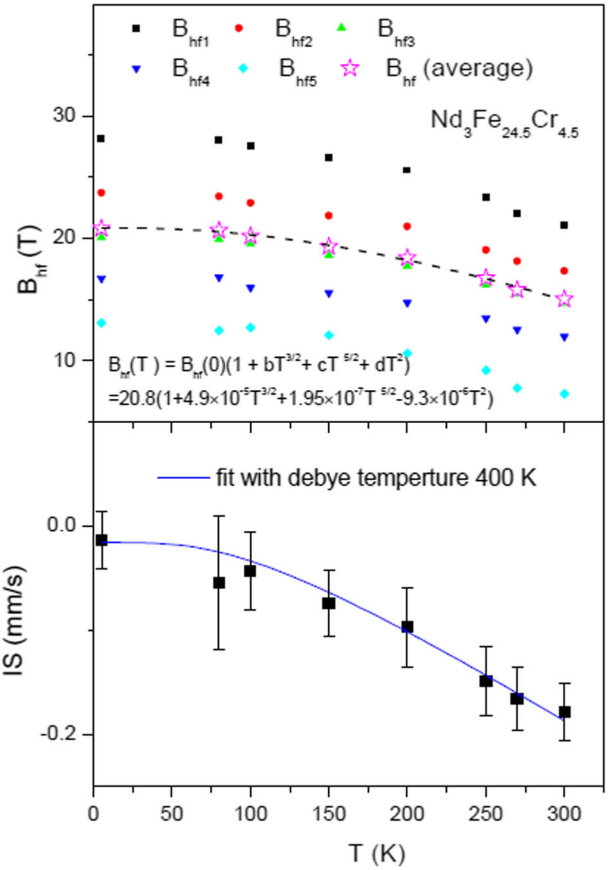

Fig. 5 The temperature dependences of: (**a**) the magnetic hyperfine field B_{hf}; and (**b**) the average isomer shift δ. The dashed line through the average isomer shift values represents the calculated result using Debye temperature $\theta_D = 400$ K

by the temperature dependence of the unit cell volume curve of Fig. 3 where the calculated thermal expansion based on the Debye model (with Debye temperature $\theta_D = 400(30)$ K; see below) is shown by the dashed line. At 80 K, the spontaneous volume magnetostriction ω has been estimated to be 9.86×10^{-3}, which is close to the values detected in Dy_2Fe_{17} [18] ($\sim 12 \times 10^{-3}$ at 130 K) and $YFe_{11}Ti$ [19, 20] ($\sim 7.8 \times 10^{-3}$ at 80 K). It is well accepted that the close relation between magnetic and lattice effects in Fe-rich rare earth compounds and strong magnetovolume effects can be understood within the classical model of itinerant ferromagnetism in which the magnetovolume effect is related to the gradient of the density of states (DOS) at the Fermi level, E_F If E_F lies in an energy region with a steep slope of the DOS curve, small changes in the position of E_F could induce large changes in the magnetic moment [19, 20].

Figure 4 shows a series of ^{57}Fe Mössbauer spectra of $Nd_3Fe_{24.5}Cr_{4.5}$ and their subspectral components sat selected temperatures. Due to the fact that the $Nd_3Fe_{24.5}Cr_{4.5}$ compound has a rather complex structure which contains eleven inequivalent Fe sites [2–6], in order to reduce the number of fitting parameters and also reproduce the main features of the spectra, we use five sextets to fit the Mössbauer spectra as suggested previously [21, 22]. The temperature dependences of the fitted Mössbauer spectral parameters are shown in Fig. 5. The average isomer shift follows behaviour typical of the second order Doppler shift. The dashed line through the average isomer shift values in Fig. 5b represents the calculated result based on a Debye model using Debye temperature $\theta_D = 400(30)$ K. The average hyperfine field as a function of temperature can be fitted well with the power law as:

$B_{hf}(T) = 20.8(1+4.9\times 10^{-5}T^{3/2}\text{-}9.3\times10^{-6}T^2+1.95\times10^{-7}T^{5/2})$.

This indicates that the excitation of spin waves (the $T^{3/2}$ and $T^{5/2}$ terms) [23] dominates the decrease in magnetization with temperature while the contribution from Stoner single-particle excitations (the T^2 term) [24, 25] is also present. This behaviour is different compared with the case reported in $R(Fe,T)_{12}$ [26] and R_2Fe_{17} [18–24]. In these compounds it was found that the weighted average hyperfine field values follow a T^2 dependence; this suggests that a single particle excitation mechanism is responsible for reduction of the 3d-sublattice magnetization with increasing temperature.

4 Conclusions

Rietveld refinement of the x-ray diffraction data for the $Nd_3Fe_{24.5}Cr_{4.5}$ compound reveals that the Cr atoms have a strong preference to occupy the three dumb-bell 4g, 4i3, and 4i4 sites. A pronounced positive spontaneous volume magnetostriction has been observed below the Curie temperature $T_C = 423(5)$ K, and the magnetism has a significant effect on the lattice parameters a, b, c, and β. The temperature dependence of the average hyperfine field has been analyzed in terms of different power laws of the reduced temperature.

Acknowledgments This work is supported in part by Discovery Grant DP110102386 from the Australian Research Council. We also thank Dr. J.A. Kimpton for his help during our experiments at the Australian Synchrotron.

References

1. Collocott, S.J., Day, R.K., Dunlop, J.B., Davis, R.L.: Proceedings of the 7th International Symposium on Magnetic Anisotropy and Coercivity in Rare-Earth-Transition Metal Alloys, Canberra 1992, p. 437
2. Sarafidis, C., Wilhelm, F., Rogalev, A., Gjoka, M., Kalogirou, O.: J. Phys. Condens. Matter **21**, 236001 (2009)
3. Kalogirou, O., Psycharis, V., Saettas, L., Niarchos, D.: J. Magn. Magn. Mater. **146**, 335 (1995)
4. Han, X.F., Pan, H.G., Liu, H.L., Yang, F.M., Zheng, Y.W.: Phys. Rev. B **56**, 8867 (1997)
5. Yelon, W.B., Hu, Z.: J. Appl. Phys. **79**, 1330 (1996)
6. Yelon, W.B., Luo, H., Chen, M., Missell, F.P.: J. Appl. Phys. **85**, 5693 (1999)
7. Yang, F.M., Nasunjilegal, B., Wang, J.L., Pan, H.Y., Qing, W.D., Zhao, R.W., Hu, B.P., Wang, Y.Z., Liu, G.C., Li, H.S., Cadogan, J.M.: J. Appl. Phys. **76**, 1971 (1994)
8. Hu, B.P., Liu, G.C., Wang, Y.Z., Nasunjilegal, B., Zhao, R.W., Yang, F.M., Li, H.S., Cadogan, J.M.: J. Phys. Condens. Matter **6**, L197 (1994)
9. Yang, D., Wang, J.L., Tang, N., Shen, Y.P., Yang, F.M.: Appl. Phys. Lett. **74**, 4020 (1999)
10. Wang, W.Q., Wang, J.L., Tang, N., Wu, G.H., Yang, F.M., Jin, H.M.: J. Appl. Phys. **90**, 1920 (2001)
11. Ibarra, M.R., Morellon, L., Blasco, J., Pareti, L., Algarabel, P.A., Garcia, J., Albertini, F., Paoluzzi, A.: J. Phys. Condens. Matter **6**, L771 (1994)
12. Chu, W.G., Rao, G.H., Yang, H.F., Liu, G.Y., Liu, W.F., Liang, J.K.: J. Phys. Condens. Matter **14**, 5035 (2002)
13. Wang, J.L., Marquina, C., Ibarra, M.R., Wang, W.Q., Yang, F.M., Wu, G.H., Tegus, O., Klaasse, J.C.P., Brück, E., de Boer, F.R.: J. Appl. Phys. **93**, 6924 (2003)

14. Han, X.F., Wang, J.L., Pan, H.G., Wang, Y.G., Liu, P., Han, B.S., Yang, F.M.: J. Appl. Phys. **81**, 5170 (1997)
15. Gelato, L.: J. Appl. Crystallogr. **14**, 151 (1981)
16. Givord, D., Lemaire, R.: IEEE Trans. Magn. **10**, 109 (1974)
17. Li, Z.W., Zhou, X.Z., Morrish, A.H.: Phys. Rev. B **51**, 2891 (1995)
18. Wang, J.L., Campbell, S.J., Tegus, O., Marquina, C., Ibarra, M.R.: Phys. Rev. B **75**, 174423-1 (2007)
19. Wang, J.L., Ibarra, M.R., Marquina, C., García-Landa, B., Tegus, O., Xiao, Q.F., Bruck, E., Yang, F.M., Wu, G.H.: J. Appl. Phys. **91**, 8216 (2002)
20. Wang, J.L., Marquina, C., García-Landa, B., Ibarra, M.R., Yang, F.M., Wu, G.H.: Physica B **319**, 73 (2002)
21. Kalogirou, O., Psycharis, V., Gjoka, M., Niarchos, D., Fuerst, C.D.: J. Appl. Phys. **79**, 5539 (1996)
22. Nagamine, L.C.C.M., Rechenberg, H.R., Han, X.F., Baggio-Saitovitch, E., Souza Azevedo, I., Lin, L.Y.: Phys. Stat. Sol. (b) **221**, 767 (2000)
23. Majumdar, A.K., Oestreich, V., Weschenfelder, D., Luborsky, F.E.: Phys. Rev. B **27**, 5618 (1983)
24. Venkatesan, M., Varadaraju, U.V., Rama Rao, K.V.S.: Phys. Rev. B **64**, 094427 (2001)
25. Patel, R.S., Majumdar, A.K., Hebard, A.F., Temple, D.: J. Appl. Phys. **97**, 033910 (2005)
26. Wang, J.L., Campbell, S.J., Cadogan, J.M., Tegus, O., Edge, A.V.J.: J. Phys. Condens. Matter **17**, 3689 (2005)